First-principles investigations of the ground-state and excited-state properties of BeO polymorphs

IOP PUBLISHING JOURNAL OF PHYSICS: CONDENSED MATTER

J. Phys.: Condens. Matter **19** (2007) 436216 (12pp) doi:10.1088/0953-8984/19/43/436216

First-principles investigations of the ground-state and excited-state properties of BeO polymorphs

Bouhalouane Amrani[1], **Fouad El Haj Hassan**[2] **and Hadi Akbarzadeh**[3]

[1] Centre Universitaire de Mascara, Mascara 29000, Algeria
[2] Laboratoire de Physique des Matériaux, Département de Physique, Faculté des Sciences, Elhadath, Beirut, Lebanon
[3] Department of Physics, Isfahan University of Technology, Isfahan 84154, Iran

E-mail: abouhalouane@yahoo.fr

Received 13 July 2007, in final form 27 August 2007
Published 1 October 2007
Online at stacks.iop.org/JPhysCM/19/436216

Abstract

An investigation into the structural stabilities and the optoelectronic properties of BeO polymorphs was conducted using first-principles calculations based on density-functional theory. In agreement with experimental and earlier *ab initio* calculations, we found that the B4 phase is slightly lower in energy than the B3 phase, and that it transforms to the B1 structure at 107 GPa, while the B3–B1 transition occurs at 110 GPa. In addition, we found that BeO has a indirect gap in the B3 structure with a band gap of 9.01 eV and a direct band gap in the B4 and B1 phases with band gaps of 8.58 and 8.12 eV, respectively. Also, we have presented the results of the effective masses. To complete the fundamental characteristics of this compound we have analyzed their linear optical properties such as the dynamic dielectric function and energy-loss function for a wide range of energies 0–35 eV.

(Some figures in this article are in colour only in the electronic version)

1. Introduction

Beryllium oxide, BeO, has a number of anomalous properties which make it an interesting material from the physics point of view [1]. It is the only alkaline-earth oxide crystallizing in the hexagonal wurtzite structure; the other alkali-earth oxides crystallize in the cubic sodium chloride (rock salt) structure. This indicates that the Be–O chemical bond is not exclusively ionic but has also some covalent character. Further, not only is BeO harder than the other alkaline-earth oxides but it is also among the hardest materials known [2]. Also, BeO has a high melting point [3], high thermal conductivity [4], high electrical resistivity [5] and high-energy band gap [6]. It has been used as a nuclear moderator in nuclear reactors [7] and as a chip carrier substrate [5] for high-power applications. For semiconductor device applications

an understanding of the geometric and optoelectronic properties under high pressure is highly desirable.

During the last two decades, a few theoretical calculations [1, 8–12] and experiments [1, 13] have been performed to investigate the pressure-induced phase transition sequence in BeO. However, a significant discrepancy exists in the magnitude of the transition pressure. Earlier first-principles pseudopotential calculations predicted that the B4 → B1 transition occurs at 22 GPa [8] and the same transition was predicted at 40 GPa by the potential-induced-breathing (PIB) method [1]. On the other hand, the latter calculations predicted that the B4 phase first transformed into the zinc blende structure (B3) and then into the B1 phase. Herein, the work of Van Camp and Van Doren using the soft nonlocal pseudopotential predicted the B4 → B3 → B1 transitions at 74 and 137 GPa, respectively [9], while Park *et al* [10], who used a first-principles soft nonlocal pseudopotential method within the generalized-gradient approximation (GGA), predicted the transition pressures to be 91 (B4 → B3) and 147 GPa (B3 → B1), respectively. By use of the full-potential linear muffin-tin orbital (FPLMTO) method, Boettger and Wills [11] have also predicted a B4 → B3 → B1 phase transition sequence at 63–76 and 95 GPa. More recently, Cai *et al* [12], by systematically calculating the enthalpy barrier of the phase transition, have shown that only the B4 → B1 transition will occur with increasing pressure. This unusual transition sequence is attributed to the large charge asymmetry and the small bond length of BeO [10]. Previous experiments examined the high-pressure behavior using vibrational Raman spectroscopy, and no phase transition was observed up to a pressure of 55 GPa [1]. The most recent static high-pressure x-ray diffraction experiment [13] also showed no phase transition up to 126 GPa, but a new phase was found at 137 GPa. With increasing pressure, the B4 phase disappeared at 175 GPa.

To the best of our knowledge there are no theoretical calculations based on the full-potential linearized-augmented-plane-wave (FP-LAPW) method. Therefore, the aim of this paper is to investigate the structural, electronic and optical properties of the ground state and excited states of BeO, by using the FP-LAPW method. The rest of this paper is organized as follows. In section 2, we briefly describe the calculation procedure and give the computational details. In section 3, we report and discuss our results for structural and optoelectronic properties of the B4, B3, and B1 phases of BeO, and P_t for the B4 (B3) → B1 transitions. Finally, conclusions are drawn in section 4.

2. Method of calculations

The first-principles calculations performed in this paper are based on density-functional theory (DFT). The total energies were calculated within the full-potential linearized-augmented-plane-wave (FP-LAPW) + local orbitals (lo) method, implemented in the WIEN2k code [14]. In this code, the crystal structures were decided under the condition that the total energy is minimized from all atomic configurations. The exchange–correlation energy of electrons is described in generalized-gradient approximation (GGA96) [15]. The Engel–Vosko (EV) approximation [16] seems to lead to better band gaps than the GGA, but it cannot give reliable total energies. Therefore, the EV-GGA was considered in our calculations of the electronic and optical properties based on the optimized structure models obtained by the GGA. In order to increase the reliability and to give a reasonable comparison, we used the same radius of the muffin-tin sphere for the same kind of atom in all of the calculations. The muffin-tin radii of Be and O were chosen as 1.3 and 1.1 au, respectively. Within these spheres, the potential is expanded in the form

$$V(r) = \sum_{\mathrm{lm}} V_{\mathrm{lm}}(r) Y_{\mathrm{lm}}(\hat{r}) \tag{1}$$

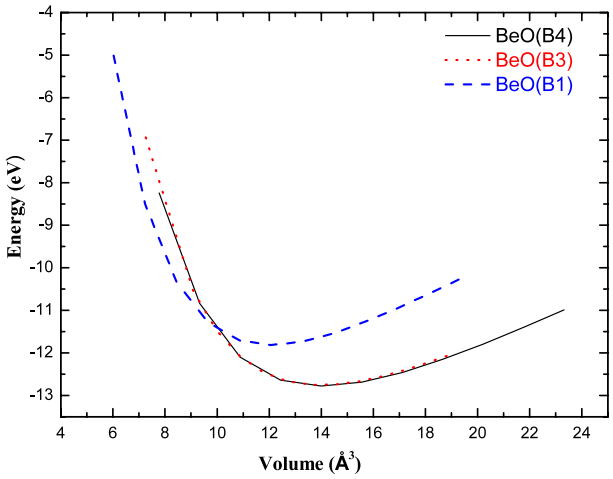

Figure 1. Calculated total energies as a function of primitive cell volume of BeO for wurtzite (solid line), zinc blende (dotted line) and rock salt (dashed line) structures.

and outside the sphere,

$$V(r) = \sum_K V_K e^{iKr}, \tag{2}$$

where $Y_{lm}(\hat{r})$ is a linear combination of radial functions times spherical harmonics. Within this calculational scheme, there are no shape approximations to the charge density or potential. The charge density was Fourier expanded up to $G_{max} = 14$ (Ryd)$^{1/2}$. The iteration process was repeated until the calculated total energy of the crystal converged to less than 0.1 mRyd/unit cell. A mesh of 35 special k-points in the zinc blende (B3) and rock salt (B1) structures and 40 special k-points in the wurtzite (B4) structure were taken in the irreducible wedge of the Brillouin zone. Both the muffin-tin radius and the number of k-points were varied to ensure total-energy convergence.

3. Results and discussion

3.1. Structural properties

Total energy versus volume data for the B4, B3 and B1 phases of BeO are shown in figure 1. Volume and energy are per single BeO formula unit in all cases. The zero of energy is taken as the sum of the energies of isolated neutral O and Be atoms, so that the absolute value of the energy E_{coh} at the minimum of each curve gives our prediction for the equilibrium cohesive energy of the corresponding phase of BeO. The curves were obtained by fitting the calculated values to the Murnaghan equation of state [17].

In agreement with earlier *ab initio* calculations and with experiment, we find that the B4 phase of BeO is slightly lower in energy than the B3 phase. The difference between the equilibrium E_{tot} of the B4 and B3 phases is very small (26 meV). This is expected, since the B4 and B3 phases have local tetrahedral bonding and they only differ in the second-nearest neighbors. The calculated structural parameters of the BeO phases are listed in table 1, compared with the available experimental data and other theoretical results. The comparison with experimental data for the B4 structure shows an overestimate of the lattice constants by less than 0.6% (2.1% in volume), whereas the ratio $(c/a)_{eq}$ is slightly overestimated (0.2%). In

Table 1. Calculated structural parameters for B4 (wurtzite), B3 (zinc blende) and B1 (rock salt) phases of BeO compared with both experimental and theoretical data reported in the literature.

Approach	E_{coh} (eV)	V_{eq} (Å^3)	a_{eq} (Å)	c_{eq}/a_{eq}	U_{eq}	B_{eq} (GPa)
			Wurtzite (B4)			
This work	12.728	14.084	2.714	1.626	0.3773	206
Experiment [2]		13.794	2.698	1.622	0.378	212
PP:LDA [9]		12.964	2.639	1.629	0.3769	227.6
PP:LDA [10]	14.395	13.086	2.650	1.624	0.378	224
PP:GGA [10]	12.953	13.853	2.703	1.620	0.377	203
FPLMTO: LDA [11]	14.068	13.429	2.668	1.633		239
LCGTO-FF:LDA [11]	14.109	13.339	2.662	1.633	0.3769	226
			Zinc blende (B3)			
This work	12.702	14.021	3.828			203
PP:LDA [9]		12.932	3.726			228.1
PP:LDA [10]	13.677	13.047	3.737			224
PP:GGA [10]	13.606	13.827	3.810			201
FPLMTO: LDA [11]	14.055	13.374	3.768			229
LCGTO-FF:LDA [11]	14.096	13.300	3.761			240
			Rock salt (B1)			
This work	11.751	12.169	3.651			232
PP:LDA [9]		11.383	3.571			266.1
PP:LDA [10]	13.470	11.442	3.577			264
PP:GGA [10]	11.878	12.137	3.648			231
PP:LDA [10]						
FPLMTO: LDA [11]	13.225	11.567	3.590			272
LCGTO-FF:LDA [11]	13.279	11.577	3.591			269

the case of the bulk modulus, B_{eq}, our results are somewhat lower than those reported in [9–11] for the LDA calculation, but agree well with the GGA result reported in [10], and are still close to the experimental value as reported in [2]. There are no experimental results available of structural properties to use for B3 and B1 phases, but our values are relatively close to those of Park *et al* [10].

As shown in figure 1, the curve of B4 is very close to B3; hence it is difficult to extract accurate slopes from the common-tangent lines between these two phases. The values of P_t of the B4 $\rightarrow$ B1 (B3 $\rightarrow$ B1) transitions of BeO were determined by calculating the Gibbs free energy (G) for the two phases (i.e., wurtzite and zinc blende) that is given by $G = E + PV - TS$. Since the theoretical calculations are performed at $T = 0$ K, the Gibbs free energy becomes equal to the enthalpy, $H = E + PV$. The enthalpy of BeO with B4, B3, and B1 structures was calculated, and the phase transition pressure was obtained from enthalpy curve crossings. Table 2 lists the calculated pressures and other related quantities. As can been seen from figure 2, the first transition (B4–B1) takes place at 107 GPa, in agreement with the calculated values reported in [11, 12]. The transition pressure for BeO from the zinc blende to the rock salt phase is found to occur at 110 GPa, in reasonable agreement with other recent theoretical results reported by Boettger *et al* [11]. On the other hand, our calculations show that there is no transformation from wurtzite to zinc blende.

3.2. Electronic properties

To study the influence of the atomic geometry, more precisely the polymorph of BeO, we have calculated the total densities of states and band structure using both the GGA and EV-GGA

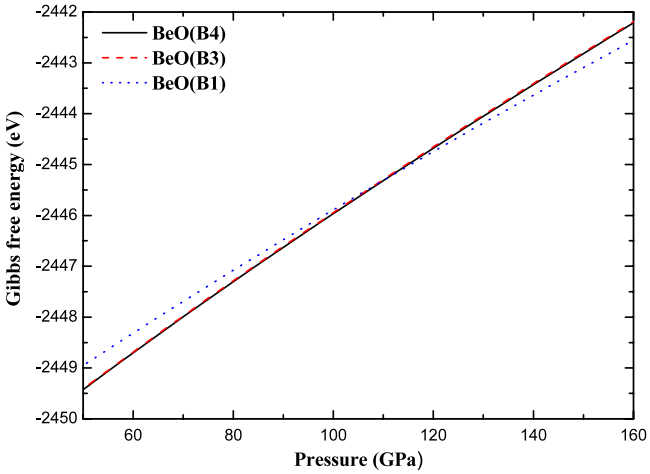

Figure 2. Gibbs free energies per formula unit at temperature $T = 0$ K for the B1, B3 and B4 phases.

Table 2. Transition pressures P_t, initial transition volumes V_t, and fractional volume changes $\Delta V/V_t$ for the wurtzite to zinc blende and zinc blende to rock salt transitions.

	This work	Other theoretical calculations
	B4 → B1 transition	
P_t (GPa)	107.39	137.3[a], 93.8[d], 95.4[e], 105[f]
V_t	10.37	9.471[a], 10.40[d], 10.37[e], 10.75[f]
$\Delta V/V_t$	0.111	−0.073[a], −0.114[d], −0.114[e], −0.102[f]
	B3 → B1 transition	
P_t (GPa)	110.33	147.1[b], 126.5[c], 94.1[d], 96.1[e]
V_t	10.32	9.45[b], 9.46[c], 10.38[d], 10.33[e]
$\Delta V/V_t$	0.113	−0.092[b], −0.096[c], −0.113[d], −0.112[e]

[a] Reference [9], using LDA: PP.
[b] Reference [10], using GGA: PP.
[c] Reference [10], using LDA: PP.
[d] Reference [11], using LDA: FPLMTO.
[e] Reference [11], using LDA: LCGTO-FF.
[f] Reference [12], using GGA: PP.

schemes for the three phases B1, B3 and B4 of BeO. The results are presented in figure 3. The GGA functionals have simple forms that are not sufficiently flexible to accurately reproduce both the exchange–correlation energy and its charge derivative. Engel and Vosko [16] by considering this shortcoming constructed a new functional form of the GGA which is better able to reproduce the exchange potential at the expense of less agreement in the exchange energy. This approach, which is called the EV-GGA, yields a better band splitting and some other properties which mainly depend on the accuracy of the exchange correlation potential. On the other hand, in this method, the quantities which depend on an accurate description of the exchange energy E_x, such as equilibrium volumes and bulk modulus, are far from experimental values. Therefore we always apply the EV-GGA for the electronic properties and the GGA for the structural properties. From the partial density of states we are able to identify the angular momentum character of the various structures. In all cases the total density of states presents

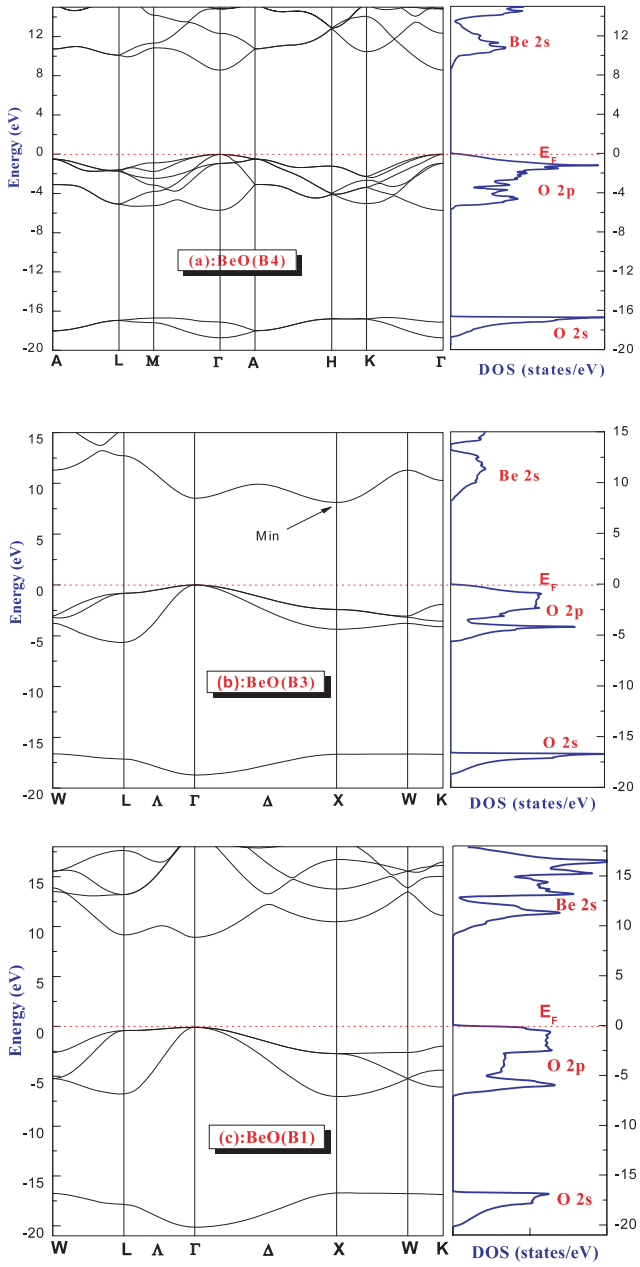

Figure 3. Band structure calculated along high-symmetry directions (using the EV-GGA) and the total density of states of BeO for the (a) wurtzite, (b) zinc blende and (c) rock salt structures.

three regions. Our calculations suggested that the lower part of the valence band is dominated by the O 2s orbital, and the upper part by the O 2p orbital in BeO. The lower part of the conduction band is dominated by the Be 2s orbital. From the band structures we find that BeO at zero pressure is a semiconductor with a direct gap of 7.444 eV in the GGA, in agreement with [20, 21], but it is much smaller than the experimental value (10.6 eV) [18]. While the band

Table 3. The band gap calculated within different approximations for the exchange–correlation potential of BeO in the B4, B3 and B1 structures, compared to the experimental and other theoretical works (all of the energies are in eV).

	This work			
	GGA	EV-GGA	Experiments	Other theoretical calculations
BeO(B4)	7.444	8.577	10.6[a], 10.63 ± 0.1[b]	7.54[c], 7.36[d], 10.50[e], 7.8[f]
BeO(B3)	6.862	8.121		6.35[f]
BeO(B1)	8.273	9.010		

[a] Reference [18].
[b] Reference [19].
[c] Reference [21], using LDA: OLCAO.
[d] Reference [20], using LDA: PP.
[e] Reference [20], using SIP: PP.
[f] Reference [22], using LDA: PP.

gap calculated using the EV-GGA is 8.577 eV at 0 GPa, as shown in table 3, also a smaller value is obtained experimentally. Recently, the nonlocal pseudopotentials which incorporate self-interaction corrections (SICs) have been applied to calculate the band gap, and they give better results, i.e., 10.50 eV [20].

Despite the energy band gap being underestimated in the DFT-GGA and DFT–EV-GGA, its high-pressure behavior can be still compared and discussed in the calculations by using the same exchange–correlation potential. The gap in the B3 phase turns out to be an indirect band gap semiconductor. The conduction band minimum located at the X-point and the valence band maxima located at the Γ-point results in an indirect band gap of 8.121 eV calculated by the EV-GGA. For the B1 structure, it was shown that BeO has a direct band gap, and the band gap value is 9.010 eV obtained by the EV-GGA. Comparing the band structures of these three phases, we found that BeO has an indirect band gap in the B3 structure and a direct band gap in the B4 and B1 structures. The band gap is the smallest in the B3 structure and is the largest in the B1 structure.

Turning to the effective masses, we are interested in studying the effective masses of electrons and holes, which are important for the excitonic properties. We have computed the effective masses of electrons and holes along the three symmetry axes $\Gamma \rightarrow$ A, $\Gamma \rightarrow$ M, and $\Gamma \rightarrow$ K for the B4 phase. For the B3 and B1 phases, we calculated the hole effective masses along the $\Gamma \rightarrow$ X, and $\Gamma \rightarrow$ L, directions. For B3 BeO, the minimum of the conduction band is at X, so the component for the electron effective masses is evaluated at the X-point. The different effective masses are obtained from the expression

$$m^* = \pm\eta^2 \left(\frac{\mathrm{d}^2 E_k}{\mathrm{d}k^2} \right)^{-1}. \tag{3}$$

Table 4 shows our calculated electron and hole effective masses components for the B4, B3 and B1 phases. It is clearly seen that the GGA values are smaller than the corresponding values within the EV-GGA. Our results calculated by the latter are similar to those found using the first-principles orthogonalized linear combination of atomic orbital method in the local-density approximation [21] for B4 BeO. From table 4, we can conclude that hole effective masses are more anisotropic. This is related to the fact that the top of the valence band is associated with the Be 2p orbitals. The holes are much heavier than the electrons, so carrier transport in BeO should be dominated by electrons.

Table 4. Calculated effective masses for the wurtzite, zinc blende, and rock salt phases (in units of free electron mass) compared with the theoretical results of [21].

		This work		
		GGA	EV-GGA	Reference [21]
BeO (B4)	$m_e^*(\Gamma \to \mathrm{A})$	0.597	0.822	0.58
	$m_e^*(\Gamma \to \mathrm{M})$	0.753	0.878	0.73
	$m_e^*(\Gamma \to \mathrm{K})$	0.826	0.785	0.75
	$m_{hh}^*(\Gamma \to \mathrm{A})$	5.110	6.771	12.01
	$m_{hh}^*(\Gamma \to \mathrm{M})$	3.836	3.412	2.44
	$m_{hh}^*(\Gamma \to \mathrm{K})$	3.082	3.209	2.44
BeO (B3)	$m_e^*(X)$	0.536	0.540	
	$m_{hh}^*(\Gamma \to \mathrm{X})$	1.407	1.442	
	$m_{hh}^*(\Gamma \to \mathrm{L})$	3.623	4.002	
BeO (B1)	$m_e^*(\Gamma)$	0.621	0.677	
	$m_{hh}^*(\Gamma \to \mathrm{X})$	1.440	1.518	
	$m_{hh}^*(\Gamma \to \mathrm{L})$	8.884	8.728	

3.3. Optical properties

The dielectric function, $\varepsilon(\omega)$, can be used to describe the linear response of the system to electromagnetic radiation, which is related to the interaction of photons with electrons. Of the two contributions to $\varepsilon(\omega)$, namely intraband and interband transitions, contributions from the intraband transitions are ignored in calculations as they have been shown to be important only for metals. The imaginary part, $\varepsilon_2(\omega)$, of the dielectric function can be calculated from the momentum matrix elements between the occupied and unoccupied wavefunctions within the selection rules, and the real part $\varepsilon_1(\omega)$ of dielectric function can be evaluated from the imaginary part $\varepsilon_2(\omega)$ by the Kramer–Kronig relationship. All the other optical constants can be derived from $\varepsilon_1(\omega)$ and $\varepsilon_2(\omega)$, such as the refractive index $n(\omega)$, and energy-loss function $L(\omega)$:

$$n(\omega) = \frac{1}{\sqrt{2}}\left[\sqrt{\varepsilon_1^2(\omega) + \varepsilon_2^2(\omega)} + \varepsilon_1(\omega)\right]^{1/2}, \tag{4}$$

$$L(\omega) = \mathrm{Im}\left(-\frac{1}{\varepsilon(\omega)}\right). \tag{5}$$

To the best of our knowledge, apart from the results reported in [21], there are no other theoretical calculations exploring the optical properties of BeO. Hence our attempt in this direction. Figure 4 shows the calculated $\varepsilon_2(\omega)$ for the three phases of BeO. Our analysis of the dielectric $\varepsilon_2(\omega)$ functions show that the threshold peaks appear at 8.6, 8.5, and 9 eV for B4, B3, and B1 respectively. These energies are related to direct transitions between the absolute fourth valence band maximum and the first conduction band minimum, Γ_v–Γ_c.

In the B4 structure, the spectral features $\varepsilon_2^{\perp}(\omega)$ and $\varepsilon_2^{\parallel}(\omega)$ are different, meaning that the optical properties of BeO in the B4 structure are anisotropic. All the band transitions which contribute to the structures of $\varepsilon_2(\omega)$ are primarily from O 2p states to Be 2s states. For the B4 structure, the main peaks, as can be seen in figure 4(a), are determined to be at 12.5 and 15.8 eV, respectively. For the B3 structure, the main peaks were calculated to be at 11.36, 13.7, 16.04, 16.88, 18.76 and 23.03 eV and for the B1 structure at 10.41, 13.46, 14.11, 16.75, 17.54, 18.9 and 20.6 eV. Figure 5 shows the real part of the dielectric functions $\varepsilon_1(\omega)$ for the three

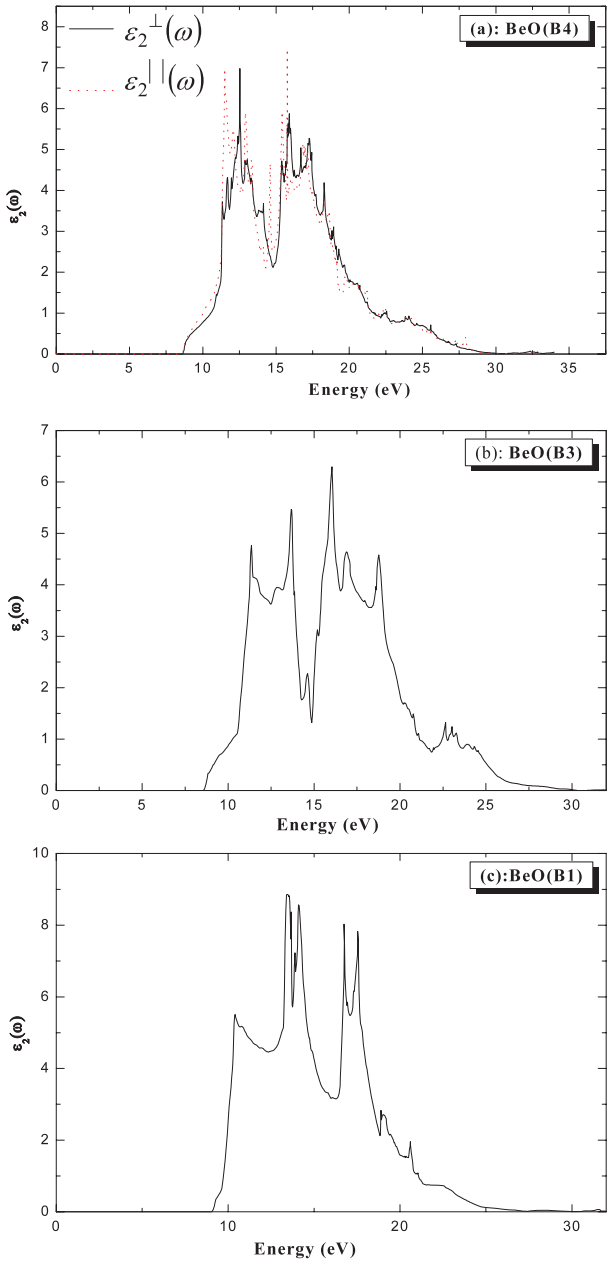

Figure 4. Imaginary part of the dielectric function for (a) the B4 structure, (b) the B3 structure, and the (c) B1 structure.

phases of BeO. The most important quantity is the zero-frequency limit ε_∞ (not including the optical phonon contribution to the screening). In the case of BeO (B4) we find $\varepsilon_\infty^{\perp} = 2.69$, and $\varepsilon_\infty^{\parallel} = 2.73$, while it is 2.7 and 3.2 for B3, and B1 respectively. This result is consistent with the data of Xu *et al* [21].

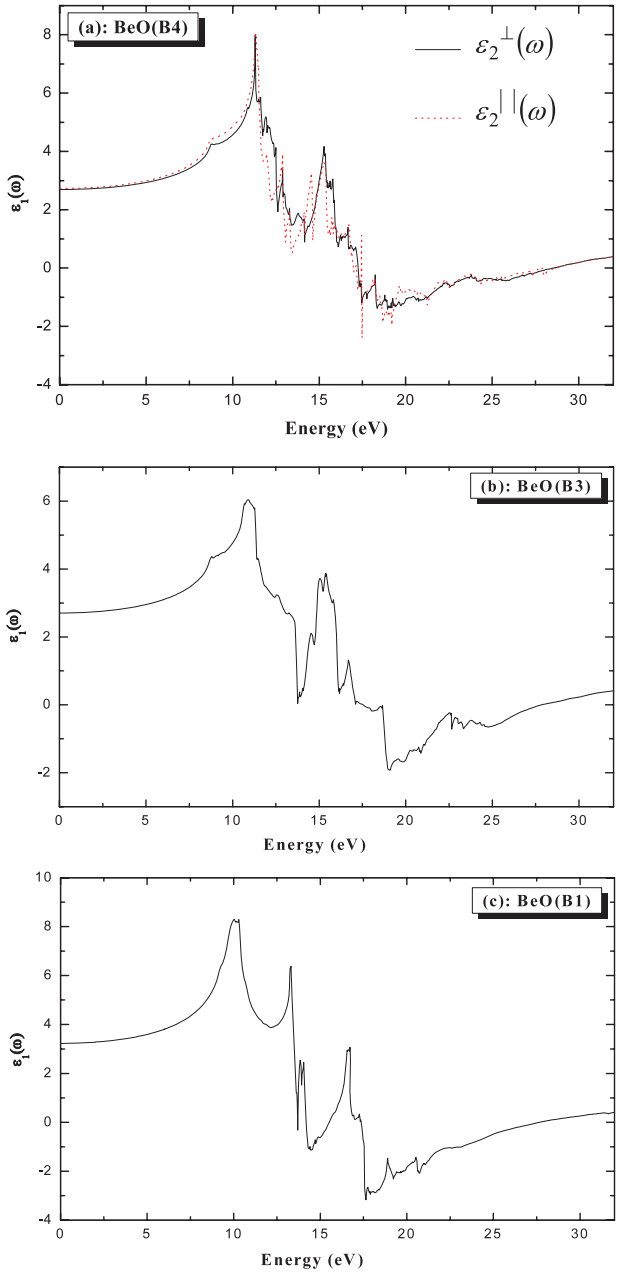

Figure 5. Real part of the dielectric function for (a) the B4 structure, (b) the B3 structure, and (c) the B1 structure.

In addition, we have also calculated the energy-loss function (as shown in figure 6); there are several features that are similar, independent of the polymorph. For the B1, B3 and B4 structures, the main peak was calculated to be at 28 eV.

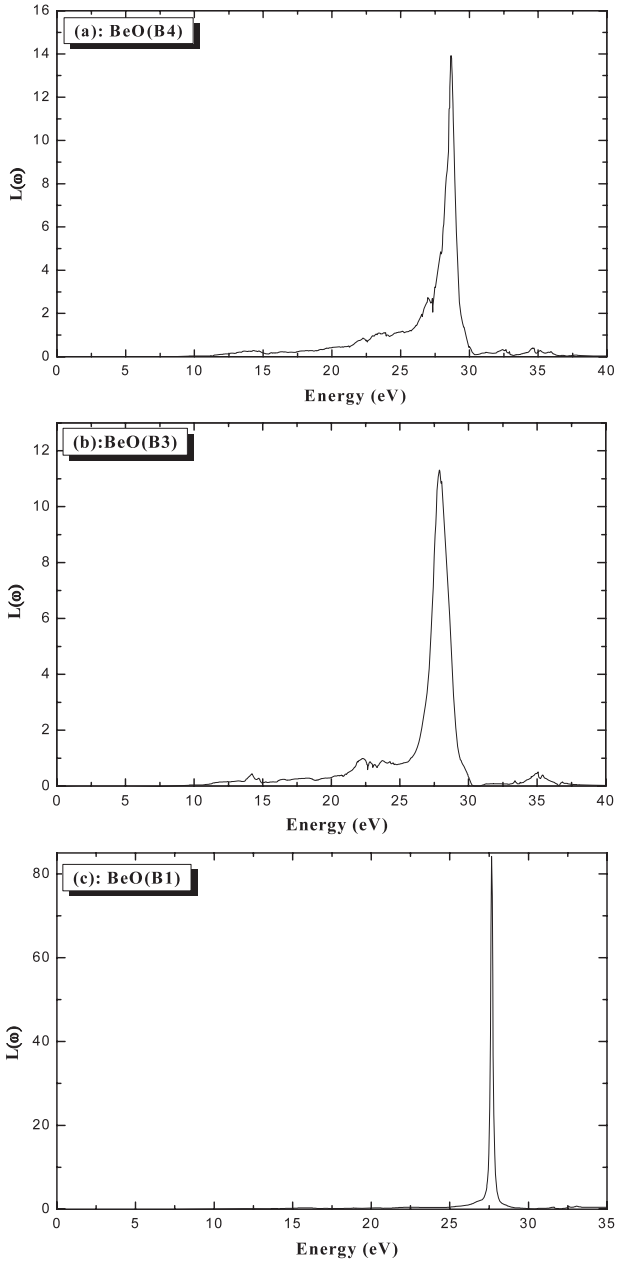

Figure 6. Energy-loss function for the (a) B4, (b) B3, and (c) B1 structures.

4. Conclusion

The structural, electronic and optical properties of BeO polymorphs have been investigated systematically using *ab initio* total-energy calculations. The equilibrium lattice constant, bulk modulus, structural phase transition, the density of states distribution and the energy band structure have all been provided. The calculated structural properties for BeO polymorphs

show excellent agreement with values reported in the literature. The B4 structure is the most stable up to 107 GPa; when the pressure exceeds this value, the phase transition will occur from the B4 to the B1 structure. The transition pressure for the transition from the B3 phase to the B1 phase is found to occur at 110 GPa. On the other hand, our calculations show that there is no transformation from B4 to B3. A density of states analysis showed that the lower part of the valence band is dominated by the O 2s orbital, and the upper part by the O 2p orbital in BeO. The lower part of the conduction band is dominated by the Be 2s orbital. From the band structures we find that BeO is a wide band gap semiconductor with a direct gap of 8.57 eV and 9 eV for the B4 and B1 phases, respectively, whereas the B3 phase turns out to be an indirect semiconductor with a band gap of 8.12 eV. We found that the results obtained from the DFT–EV-GGA method are generally in better agreement with the experimental value than other theoretical calculations. In addition, we have computed the effective masses of the electrons and the holes and compared them with the available theoretical results. To complete the fundamental characteristics of this compound we have analyzed their linear optical properties for a wide range of energies 0–35 eV. The dielectric function of the B4 phase show considerable anisotropy between the two components. All the band transitions which contribute to the structures of $\varepsilon_2(\omega)$ are primarily from O 2p states to Be 2s states.

Acknowledgment

BA acknowledges the Physics Department of Isfahan University of Technology (IUT) as an ICTP affiliated center for financial support and for their kind hospitality during the realization of this work.

References

[1] Jephcoat A P, Hemley R J, Mao H K, Cohen R E and Mehl M J 1988 *Phys. Rev.* B **37** 4727
[2] Hazen R M and Finger L W 1986 *J. Appl. Phys.* **59** 3728
[3] Weast R C (ed) 1986 *Handbook of Chemistry and Physics* 67th edn (West Palm Beach, FL: CRC Press)
[4] Slack G A and Austerman S B 1971 *J. Appl. Phys.* **42** 4713
[5] Shinozaki S S, Hangas J and Maeda K 1988 *Electronic Packaging Materials Science III* (*MRS Symposia Proceedings No. 108*) ed R Jaccodine, K A Jackson and R C Sundahl (Pittsburgh, PA: Materials Research Society) p 89
[6] Roessler D M, Walker W C and Loh E 1969 *J. Phys. Chem. Solids* **30** 157
[7] Loh E 1968 *Phys. Rev.* **166** 673
[8] Chang K J, Froyen S and Cohen M L 1983 *J. Phys. C: Solid State Phys.* **16** 3475
[9] Van Camp P E and Van Doren V E 1996 *J. Phys.: Condens. Matter* **8** 3385
[10] Park C J, Lee S G, Ko Y J and Chang K J 1999 *Phys. Rev.* B **59** 13501
[11] Boettger J C and Wills J M 1996 *Phys. Rev.* B **54** 8965
[12] Cai Y, Wu S, Xu R and Yu J 2006 *Phys. Rev.* B **73** 184104
[13] Mori Y, Ikai T and Takarabe K 2003 *Photon Factory Activity Report* vol 20B, p 215
[14] Blaha P, Schwarz K, Madsen G K H, Kvasnicka D and Luitz J 2001 *WIEN2k, An Augmented Plane Wave Plus Local Orbitals Program for Calculating Crystal Properties* Karlheinz Schwarz Techn. Universitãt Wien, Austria, ISBN: 3-9501031-1-2
[15] Perdew J P, Burke S and Ernzerhof M 1996 *Phys. Rev. Lett.* **77** 3865
[16] Engel E and Vosko S H 1993 *Phys. Rev.* B **47** 13164
[17] Murnaghan F D 1944 *Proc. Natl Acad. Sci. USA* **30** 5390
[18] Weber M J (ed) 1986 *Handbook of Laser Science and Technology* vol III (Cleveland, OH: CRC Press)
[19] Roessler D M, Walker W C and Loh E 1969 *J. Phys. Chem. Solids* **30** 157
[20] Baumeier B, Krüger P and Pollmann J 2007 *Phys. Rev.* B **75** 045323
[21] Xu Y N and Ching W Y 1993 *Phys. Rev.* B **48** 4335
[22] Chang K J and Cohen M L 1984 *Solid State Commun.* **50** 487